Biomedical Signal Processing and Control 29 (2016) 44–52

Contents lists available at ScienceDirect

Biomedical Signal Processing and Control

journal homepage: www.elsevier.com/locate/bspc

A new approach to fully-reversible watermarking in medical imaging with breakthrough visibility parameters

Aleš Roček[a,*], Karel Slavíček[b], Otto Dostál[b], Michal Javorník[b]

[a] Faculty of Electrical Engineering and Communication, Brno University of Technology, Technická 3058/10, 616 00 Brno, Czech Republic
[b] Institute of Computer Science, Masaryk University, Botanická 68, 602 00 Brno, Czech Republic

ARTICLE INFO

Article history:
Received 11 February 2016
Received in revised form 19 April 2016
Accepted 19 May 2016
Available online 10 June 2016

Keywords:
Communication
DICOM
Medical images
Security
Watermarking
Visual cryptography
RONI

ABSTRACT

Securing of medical images against intentional or accidental modification is a general issue in modern radiology. Watermarking, with its data-centric security, is very convenient for this purpose. We proposed a new method of fully reversible watermarking in medical imaging by combining the advantages of three traditional approaches—Reversible, Zero and RONI watermarking. The new method achieves exceptionally high values of Peak Signal to Noise Ratio and Structural Similarity index. The article evaluates the pros and cons of current methods of watermarking in medical imaging. Keeping the pros and eliminating the cons of the methods allows a new approach. Specific methods are selected and their application in practice described in detail. Application of the proposed method on a database of 6000 medical images from common hospital operations delivers very promising results which are discussed at the end of the article.

1. Introduction

Digital watermarking, a technique of inserting additional information into digital data, is widely used in today's digital world to secure data (It is difficult to find and remove this information from watermarked files). As medical image data processing is almost fully digitalized in healthcare institutions these days, to ensure the security of digital data is of very high importance.

Watermarking brings the undeniable advantage of security embedded directly into the data itself (i.e. Image Centric Security), which ensures the inseparability of data and the security measures. Medical image processing can be very sensitive, even on very slight changes in the image visual appearance. Modification of even a single pixel in the medical image may in some cases affect the overall information contained in the image, and so might influence the diagnosis and consequently might threaten the health or even the life of the patient. Therefore, it is necessary to approach watermarking in the area of medical imaging quite differently compared to the other areas of interest.

Section 2 of this article describes the good and bad features of the most common watermarking methods used to secure medical image data. Section 3 then proposes a new method of connecting the advantages and eliminating the disadvantages of Zero and Reversible watermarking. Section 4 describes the detail and practicalities of the Zero watermarking method used for the insertion and removal of watermarks in Regions of Interest (ROI). Section 5 contains details and a practical description of the Reversible watermarking method used in Regions of Non-Interest (RONI). Section 6 explains the principle of connection and data exchange between both sub-methods. In last section, there are experimental results of the new method and comparisons with other methods.

2. Principal problems of watermarking in the field of medical imaging

Watermarking has many advantages. Among the most important is the direct insertion of security measures into the data, called *Data Centric Security*. Security is directly present in the secured data and without knowing the right algorithms, is unrecoverable. Another advantage is that it is not directly obvious that data are secured. Nevertheless, watermarking is not deployed in common practice, because each method has its limitations, as described above. From the description below and comparison of the most common methods of watermarking of medical images [1] arise problems which make their use difficult or completely exclude them from everyday operation in medical practice [2].

* Corresponding author.
E-mail addresses: xrocek00@stud.feec.vutbr.cz (A. Roček), karel@ics.muni.cz (K. Slavíček).

http://dx.doi.org/10.1016/j.bspc.2016.05.005

2.1. Watermarking in RONI

The change of a single bit in a medical image could be a problem for correct diagnosis. Using RONI-only watermarking, watermarks are stored only in parts that do not contain information important to diagnosticians. Selection of the RONI (Region of Non-Interest) can be either automatic or manual. The reliability of automatic detection of important areas depends on the chosen method. In practice, different methods of automatic RONI selection are mostly used [3–5]. There is considerable similarity to previously-known watermarking methods applied to the RONI area, but on the other hand, there is a lack of protection in the part of the medical image that is most important. The need to search RONI makes watermarking more difficult and can cause errors with both automatic and manual ROI labeling processes.

2.2. Reversible watermarking

Reversible watermarking is based on the process of watermark insertion into a medical image, transmission of the watermarked image, and the complete removal of the watermark from the image on the recipient's side. After watermark removal, the original image is completely restored and unchanged. Once the watermark is removed from the image, the image is no longer protected. Evidently, there is a requirement to transmit those differential values in a secure way. These differences are used at the recipient's side to remove the watermark and reconstruct the original image [6–10]. As an advantage of this method, we can mention the possibility of securing the whole image by robust watermarking methods and higher capacity than RONI watermarking. The major disadvantage is the need to create another channel for secure transport of differential information.

2.3. Zero watermarking

In zero watermarking, a watermark is not inserted directly into the watermarked data, but is kept separate for later comparison. As a result, it can be considered as a lossless since no data are modified. It is primarily used to ensure copyrights protection. It is based on a Certification Authority (CA) [5,10].

The main advantages are high robustness and zero distortion of the watermarked image. The big disadvantage is the need to build a fairly complex CA system for watermark storage and comparison.

2.4. Watermarking with image change not affecting diagnosis

Methods which change the values of some bits in the resulting image can also be used for watermarking of medical images. However, the change has to be so insignificant that it cannot in any way affect the final diagnosis that the study was intended for. In general, this method can be used with images obtained using scanning modalities with a higher resolution than is needed for accurate diagnosis. This type of watermarking is typically suitable for X-ray images such as fractures, where important information is seen from surrounding pixels, regardless of the exact shade of grayscale in the given bit depth. This method is unsuitable for images intended for the diagnosis of metastasis for which accurate bit pixel value as well as its surroundings is critical [11].

3. Proposed concept: a combination of Zero and Reversible watermarking

By suitably combining particular methods in the right way, the disadvantages of each method will be eliminated and their strengths emphasized. This could remove the last obstacle to the use of watermarking in practice to secure medical images.

The proposed method consists of the combination of Zero, Reversible and RONI watermarking. The basic idea is that the image is divided into two parts: ROI and RONI. RONI is the part of the image where small changes do not distort medical information. ROI is the rest of the image.

Detection of RONI on a representative sample of medical images (from a database of more than 60 000 images) was carried out in study [20]. Finding the RONI is done automatically. The detection method is based on comparing pairs of neighboring vectors. Vectors contain pixel values of rows and columns. The comparison is made in each direction – from top, bottom, right and left – from the edges to the center of the image. Along each vector, the border between ROI and RONI is the place on the vector which differs from the previous point by more than the specified threshold. In the study, the threshold was defined as 10% similarity, after practical tests. Detailed information can be found in Ref. [20]. More accurate determination of RONI taking into account object contours, as in Ref. [21], is not a subject of this research. This study proved that all examined medical images, which we consider to be a representative sample of medical imaging, have a RONI of size 11% or more of the whole image. This is sufficient for the proposed method, in which it is calculated with 10% of RONI.

The size of ROI is expected to be significantly greater than RONI (80–90%). The ROI is secured by Zero watermarking. The information needed to remove the watermark from the secured ROI is called the *Secret Share*, which is embedded as a watermark into RONI using Reversible watermarking, which must have high capacity due to its size. This secures the image without changing its most important parts, and allows complete reconstruction of the original image as well as verification of its authenticity.

Watermark extraction and reconstruction of the original image includes: extraction of the Secret Share by Reversible watermarking as a watermark from RONI; calculating the *Public Share* with Zero watermarking in ROI; and joining them into the original watermark. Then, the original image data in the RONI region is reconstructed with Reversible watermarking and connected with the unchanged ROI in its original form.

The main advantage of this method is securing not only RONI, but also the most valuable part of the image—ROI. This major part of the picture is protected in its original form with Zero watermarking. Furthermore, this solves the problem of creating a special secure information channel, which is necessary in Reversible watermarking. This channel is made by hiding information necessary to extract the watermark with Zero watermarking in RONI. The main watermarking methods' property space, and the locations of ROI and RONI watermarking, are shown in Fig. 1.

While for watermarking in ROI, imperceptibility and robustness are essential, for watermarking in RONI, capacity and possibly robustness are particularly important.

4. Implementation of Zero watermarking in ROI in the context of the proposed concept

The watermarking method for ROI is based on the Zero watermarking principle. It came out of the method described in Ref. [12], which combines the robustness of watermarking using dual-tree complex wavelet domain and the benefits of visual cryptography.

It consists of three parts: the concealment process, the extraction process and watermark reduction. The process of watermark hiding uses Dual Tree Complex Wavelet Transform (DT-CWT) [13] to create a binary matrix B based on the low-low (LL) sub-band coefficients. From the matrix B and the watermark, the Secret Share is then generated using visual cryptography.

The same procedure is used for removing the watermark to generate a Public Share. After overlapping (logical OR) the Secret and

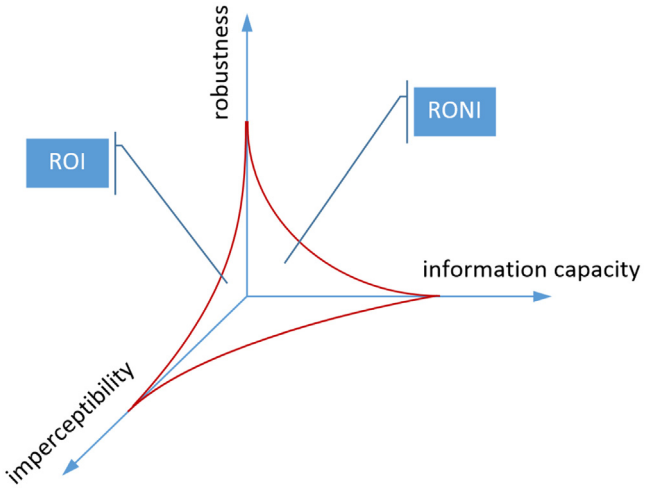

Fig. 1. Main property space of watermarking methods and location of ROI and RONI watermarking.

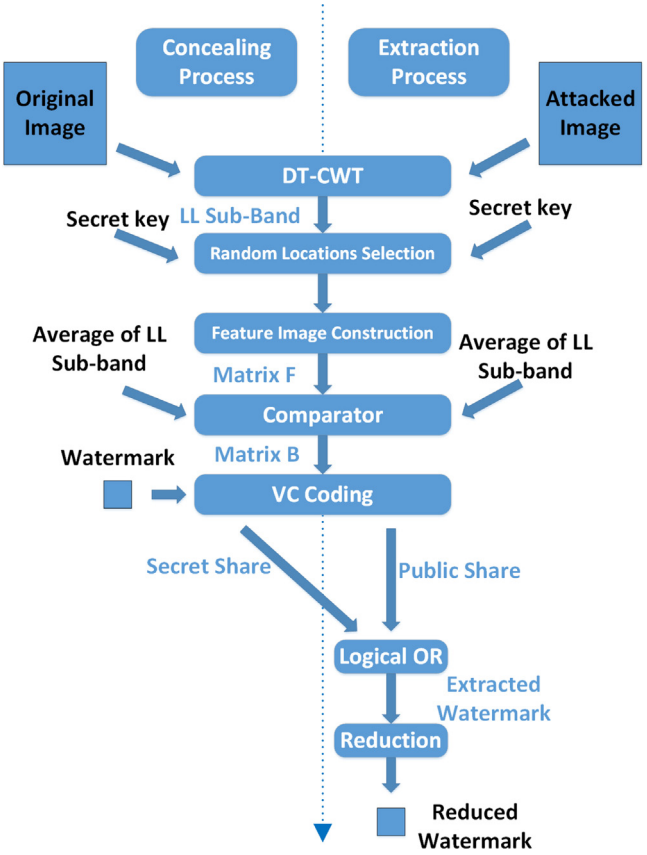

Fig. 2. Concealing and extraction of watermark in ROI.

Public Shares (which is typical for visual cryptography) and reduction, the watermark is obtained as a result. The entire process is shown in Fig. 2.

4.1. Concealment of watermark in ROI

1. ROI is selected from the original image—Fig. 3.
2. DT-CWT transform of ROI is carried out and LL sub-band of DT-CWT coefficients is selected (Fig. 4).
3. Calculate arithmetic average of LL coefficients $\emptyset_{LL}$.

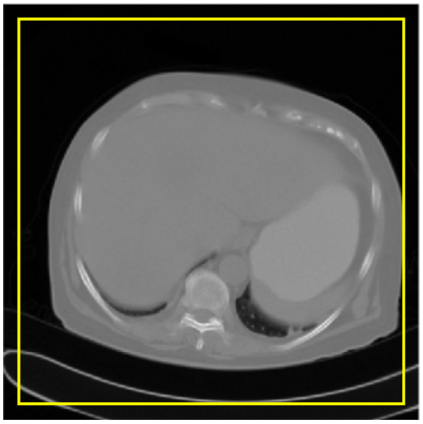

Fig. 3. ROI selection.

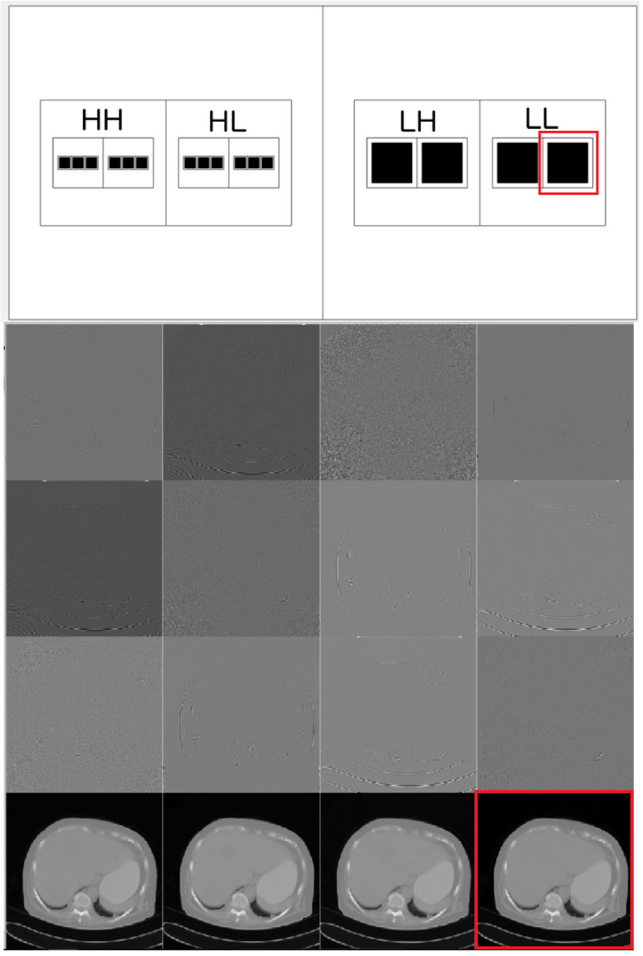

Fig. 4. LL sub-band of DT-CWT coefficients.

4. Use the secret key S as a seed (number used to initialize pseudo-random generator) to determine the random location of pixels within the LL coefficients region. The number of locations is equal to the number of pixels in the watermark. Let R_i (x, y) be the i-th random location. This location must not be closer than 4 points to the edge of the image—Fig. 5.
5. For each location R_i (x, y) a neighboring region of 7×7 pixels is selected, centered on R_i (x,y). The average of the area is calculated.

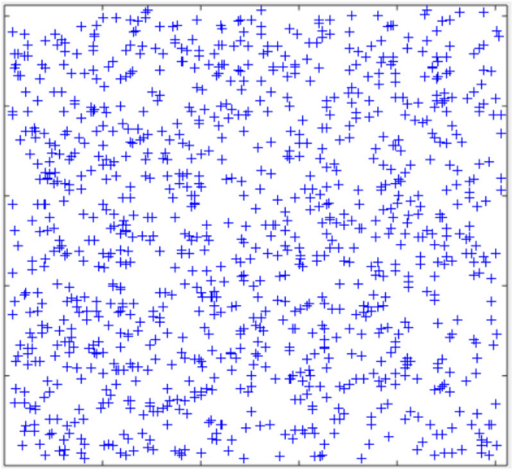

Fig. 5. Random pixel locations within LL sub-band.

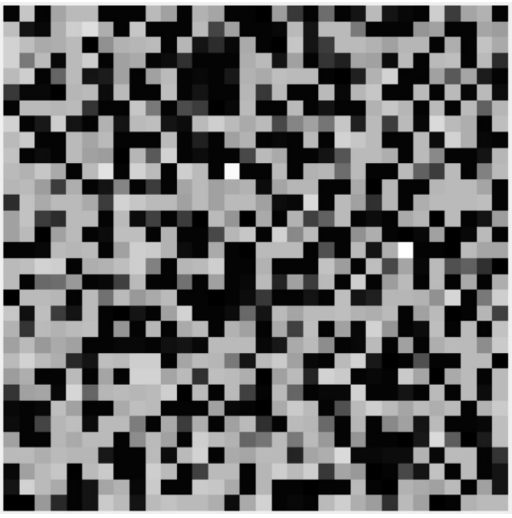

Fig. 6. Feature image F.

Table 1
Codebook used to generate Public Share and Secret Share.

Pixel				
Matrix B	0	1	0	1
Public Share	■□	□■	■□	□■
Secret Share	■□	□■	□■	■□
Public Share ⊕ Secret Share	■□	□■	■	■

6. Create feature image F with size of inserted watermark, which contains the individual averages obtained in the previous step (Fig. 6).
7. According to the Formula (1) binary matrix B (Fig. 7) is created from Feature Image F:

$$B(x,y) = \begin{cases} 1, if F(x,y) \geq \emptyset_{LL} \\ 0, if F(x,y) < \emptyset_{LL} \end{cases} \quad (1)$$

8. By combining matrix B and a watermark according to Table 1, a Secret Share is obtained which has twice as many points as the embedded watermark Fig. 8.
9. This Secret Share is used as a watermark to RONI.

Fig. 7. Binary matrix B.

Fig. 8. Secret Share.

Fig. 9. Public Share.

4.2. Extraction of watermark in ROI

1. ROI is selected from the watermarked image.
2. DT-CWT transform is carried out with RONI and LL sub-band of coefficients is selected.
3. Arithmetic average $\emptyset_{LL}$ of LL coefficients is calculated.
4. Secret key S is used as a seed to generate same random pixel location within LL coefficients as in a concealing process.
5. For every $R_i(x,y)$ location, a neighbor area 7×7 pixels centered on $R_i(x,y)$ is chosen. The average of the area is calculated.
6. Create feature image F with size of inserted watermark, which contains the individual averages obtained in the previous step.
7. Binary matrix B is created according to Formula (1).
8. Combining matrix B and Table 1 results in the creation of the Public Share (Fig. 9).
9. For non-reduced watermark extraction, logical OR with Secret share (obtained as a watermark from RONI) and Public Share is calculated (Fig. 10).

Fig. 10. Extracted watermark.

Fig. 11. Reduced extracted watermark.

10. The watermark is reduced to its original size by using Table 2.

The watermarked and original images are identical: watermark (Fig. 11) is 100% extracted.

5. Implementation of Reversible watermarking in RONI in the context of the proposed concept

When choosing a reversible watermarking method, one must carefully consider its capacity, which is from the principle of method depended on the ratio of ROI/RONI. The greater the size of ROI, the greater the capacity of the methods needed in RONI. Dependence of necessary capacity [bit/pixel] on the area of ROI is shown in Fig. 12.

A study of RONI size made over a large database of commonly used medical images showed that it is possible to count that RONI exceeds 11% of the image size. It was therefore necessary to choose a method that had a greater capacity than 0.04bits of watermark to 1 image pixel on a 512×512 image.

As described below, the proposed method works even when the RONI size is 10%.

Table 2
Reduction process.

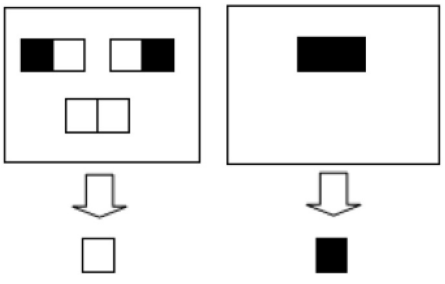

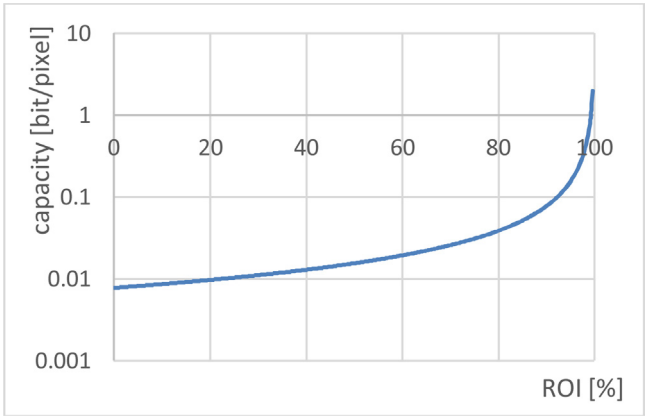

Fig. 12. Dependence of necessary capacity of watermarking on the area of ROI.

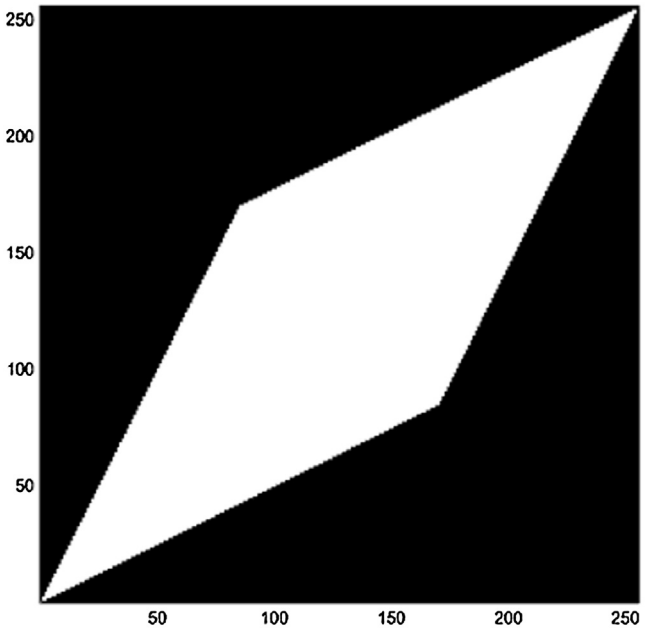

Fig. 13. Diamond shaped D domain.

The most suitable method, chosen due to its high capacity, resistance to trimming, the transparency of the reversible process and the rate of computation, was Very Fast Watermarking by Reversible Contrast Mapping [14]. During RCM (Reversible Contrast Mapping), the image is split into couples of pixels, called pairs. These pairs are used for the transformation:

$$x' = 2x - y, y' = 2y - x, \tag{2}$$

where (x, y) are the values of pairs of pixels and (x', y') are the transformed values of the pixels. To prevent overflow and underflow, the transformation is limited by sub-domain $D \subset [0, L]\,x\,[0, L]$ defined by the equations:

$$0 \le 2x - y \le L, 0 \le 2y - x \le L, \tag{3}$$

where L is grayscale (e.g. $L = 255$ for 8-bit images). As seen in Fig. 13, D is a diamond-shaped area diagonally localized in $[0, L]\,x\,[0, L]$.

The inverse transformation is defined by the equations:

$$x = \frac{2}{3}x' + \frac{1}{3}y', y = \frac{1}{3}x' + \frac{2}{3}y', \tag{4}$$

where $\lceil a \rceil$ is the ceiling function (the smallest integer greater than or equal to a).

Forward and inverse transformations can give accurate results even if the Least Significant Bits (LSB) of transformed pixels are lost, except when LSB of x' and y' are 1. From Eq. (2) it follows that this can occur only if x and y are odd. If x' and y' are not modified, Eq. (4) returns accurate results even without the ceiling function. For watermarking, it is thus possible to use the LSB of x' and y' in the case that x and y are not both odd.

Reversible watermarking based on RCM replaces the least significant bits of the transformed pairs of pixels. LSB of the first point of each pair is used to indicate whether the pair is transformed or not. A value of 1 indicates that it is, value 0 indicates that it is not. Inverse RCM fails if both values $(x, y) \in D$ are odd. Such a pair may be used to hide data in case that it is correctly identified during extraction. This can be accomplished simply by setting LSB of the first pixel to "0". During extraction LSB of both pixels are set to "1" and (3) are verified. If (3) are true, the pair was composed of odd pixels. To prevent irregularities, it is necessary to exclude pairs on borders of D. These are described by equations that are solved with pairs of odd pixels:

$$\begin{aligned} 2x - y &= 1, \\ 2y - x &= 1, \\ 2x - y &= L, \\ 2y - x &= L. \end{aligned} \tag{5}$$

There are only 170 such pairs for $L = 255$. Let Dc be the transformed domain without pairs on borders of D.

5.1. The process of watermark embedding in the RONI region

1) RONI is divided into pairs of pixels—pairs (x,y). E.g. the rows, columns, or other surface-filling curve.
2) For every pair (x, y):

a) If $(x, y) \in D$ and if it is not composed of the odd values of pixels, pair is transformed according to Eq. (2). LSB of x' is set to "1" and LSB of y' is possible to use for data insertion.
b) If $(x, y) \in D$ and if it is composed of the odd values of pixels, LSB of x is set to "0" and LSB of y' is possible to use for data insertion.
c) If $(x, y) \notin D$ LSB of x is set to "0" and real value is stored.

3) Watermark is inserted into RONI by overwriting of bits, identified in 2a and 2b by bits of watermark and bits stored in 2c.

Stored LSB bit of untransformed pair is inserted into the next free LSB of transformed pair. Thanks to that is information needed to reconstruct of original pair of pixels stored directly in it or in its immediate proximity. This procedure ensures some robustness against cropping.

5.2. The process of watermark extraction and original RONI reconstruction

1) RONI is divided into pairs of pixels (x', y').
2) For every pair (x', y'):

a) If LSB of x' is "1", LSB of y' is extracted and stored into watermark sequence. LSB of x' and y' is set to "0" and with inverse transform (4) is reconstructed original pair (x, y).
b) If LSB x' is "0", and pair (x', y') with LSB set to "1" is in D_c, LSB of y' is stored into watermark sequence and original pair is reconstructed by setting LSB (x', y') to "1".
c) If LSB of x' is "0", and pair (x', y') with LSB set to "1" is not in D_c, original values are reconstructed by replacing of LSB x' with the corresponding value from watermark sequence.

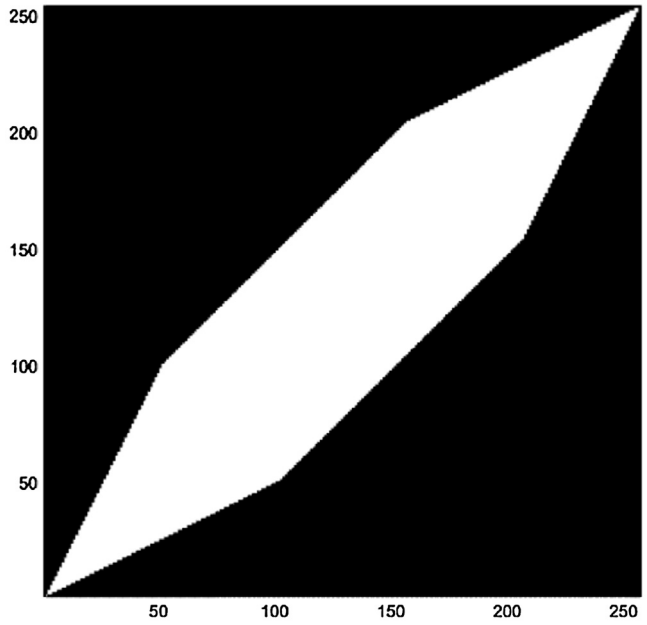

Fig. 14. Intersection of domains D and Δ.

5.3. Capacity of hiding data

Let P be the total number of pairs and T the number of pairs with stored data. This method provides T bits of space for the insertion of data. In addition to the custom watermark, it is also needed to insert LSB of first pixel of other P-T pairs. This means that there are $2T$-P bits for insertion. Capacity B of method is:

$$B = \frac{2T - P}{2P} [\text{bit/pixel}]. \tag{6}$$

This method is possible to use if at least half of the total number of pairs fulfils $T>$. The upper limit the capacity of the method B_u will be reached in the case that T, the number of pairs with stored data, will be very high and will be close to P

$$(T \approx P) : B_u = 0.5\text{bit/pixel}. \tag{7}$$

5.4. Watermarking distortion management

In cases where low distortion of the watermarked image is essential and there is no need to insert data of size approaching the capacity of the method described in RONI watermarking, it is possible to implement distortion management. The straightforward way to do this is in the transformation of pairs of pixels only if a certain threshold is not exceeded by the transformation. The error resulting from the transformation of pixel x is:

$$x' - x = 2x - y - x = x - y. \tag{8}$$

Similarly, the error resulting from the transformation of pixel y is:

$$y' - y = y - x. \tag{9}$$

Let δ be the redefined threshold. Watermarking distortion management mechanism is based on inequation:

$$|x - y| < \delta, \tag{10}$$

The pair (x, y) is transformed only in the case when in Eq. (10) is true. This inequation defines a strip domain Δ, lying on the diagonal $[0, L] \times [0, L]$. Then the RCM domain is defined by the intersection of D and Δ, $D \cap \Delta$, as shown in Fig. 14.

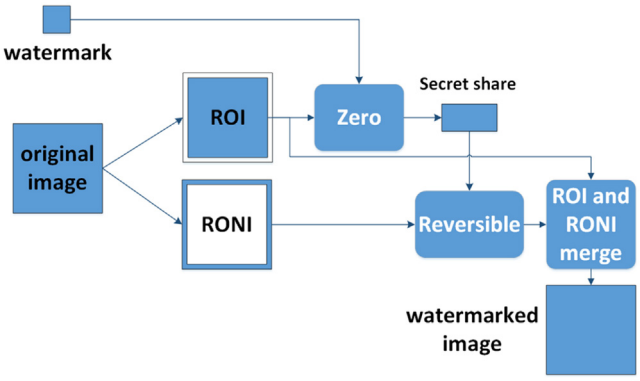

Fig. 15. Process of watermark embedding.

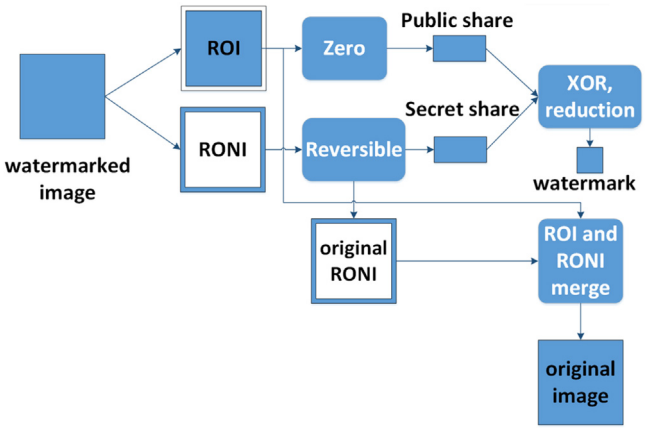

Fig. 16. Process of watermark extraction.

For watermarking distortion management during insertion and extraction of the watermark in RONI, it is only necessary to adjust the transformation domain (including the elimination of odd pairs prone to ambiguity) while introducing the error threshold. Verification of each pair slightly increases the mathematical complexity of the method.

6. Efficient interconnection of Zero and Reversible watermarking methods

6.1. The process of embedding a watermark using the Zero-Reversible method

Input data for watermark embedding:

- original medical image
- watermark

The output of watermark inserting process:

- watermarked image

The process of watermark insertion comprises the following steps (see Fig. 15):

1. The original image is divided into an area ROI (90% of the overall picture, i.e. 486 × 486) and the rest of image—RONI. For testing, grayscale images of 512 × 512, 8–16-bit depth, were used.
2. ROI and watermark (32 × 32, binary) is used for generation of Secret Share (32 × 64, binary) by Zero watermarking (see Section 4.1).
3. The Secret Share is used as a watermark in Reversible watermarking in RONI (see Section 5.1).
4. The original ROI and RONI with watermark are connected into a secure watermarked image.

6.2. The process of watermark extraction with Zero-Reversible method and original image reconstruction

Input data for watermark extraction:

- watermarked image

The output of watermark extraction and original image reconstruction:

- watermark
- original image

The process of watermark extraction and original image reconstruction comprises the following steps (see Fig. 16):

1. Watermarked image (512 × 512, 8–16-bit depth, grayscale) is divided into the 486 × 486 ROI and rest of image (RONI) areas.
2. With reversible watermarking, the watermark – Secret Share (32 × 64) – is extracted from the RONI.
3. With reversible watermarking, the original RONI is reconstructed.
4. Using zero watermarking, the Public Share (32 × 64) in ROI is calculated.
5. Using the XOR function, the watermark (32 × 64) is calculated from the Public Share and the Secret Share, which after reduction (see. Section 4.2) corresponds to the original watermark (32 × 32).
6. By merging the reconstructed RONI from point 3 and the ROI, the original image is obtained.

7. Experimental results

Implementation of method was made in the Matlab R2015a environment. Computational resources were provided by the CERIT Scientific Cloud.

7.1. Tested parameters

The fundamental attribute for watermarking of medical image data is invisibility. It is measured either by exact parameters, with a purely mathematical approach – Peak Signal to Noise Ratio (PSNR) (11) – or with consideration to the properties of the human eye—Structural Similarity Metric Index (SSIM) (12) [15,16].

$$\mathrm{PSNR} = 10\log\frac{X^2}{\frac{1}{N_1N_2}\sum_{i=1}^{N_1}\sum_{j=1}^{N_2}(C_O(i,j)-C_W(i,j))^2}, \tag{11}$$

where N_1 a N_2 are horizontal and vertical dimensions of the image, X is the maximum pixel value (in 16-bit images it is 65536), C_O is the original image and C_W is the watermarked image.

Unlike other objective methods, SSIM works with the structural layout of the measured data. Expressing similarity should therefore correspond to how the human eye perceives differences. The method works on the assumption that the brightness of the object surface is the product of light and reflection, but the structure of objects is independent of brightness. The aim of the SSIM method's creators is to suppress the effects of illumination on the data-similarity results. The SSIM index has values from −1 to 1, is

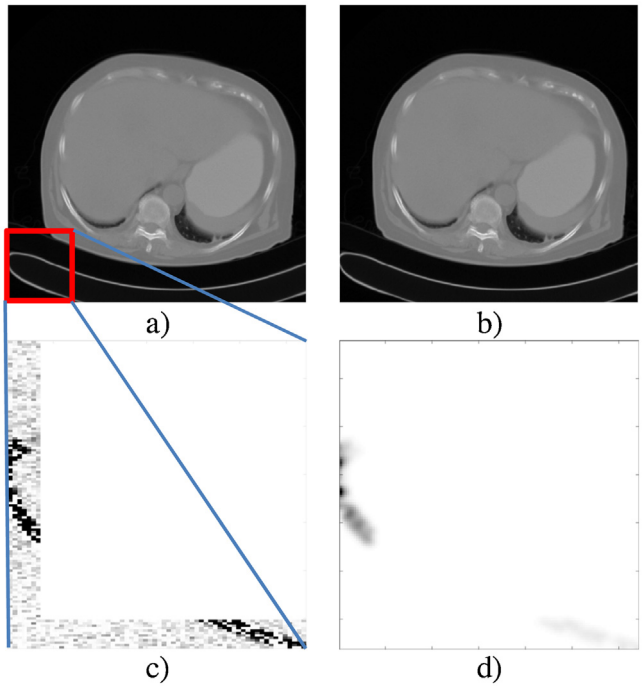

Fig. 17. (a) Original image O (b) watermarked image (c) bottom left corner of difference between the original and watermarked images (d) bottom left corner of SSIM index map.

calculated only for the brightness component, and is represented by the equation:

$$\mathrm{SSIM}(x,y) = \frac{(2\mu_x\mu_y + C_1)(2\sigma_{xy} + C_2)}{(\mu_x^2 + \mu_y^2 + C_1)(\sigma_x^2 + \sigma_y^2 + C_2)}, \tag{12}$$

where x and y are the original and modified data, μ is the average of luminance values, σ is the root mean square of the variance, σ_{xy} is the covariance, C_1 is a constant included to avoid instability when $\mu_x^2 + \mu_y^2$ is very close to zero, and C_2 is a constant included to avoid instability when the $\sigma_x^2 + \sigma_y^2$ is very close to zero.

7.2. Distortion

A watermarking example and distortion representation is shown in Fig. 17:

a) Original image O;
b) Watermarked image W;
c) Difference between the original and watermarked image O-W;
d) SSIM index map.

7.3. Test on large database of medical images

As we provide services for hospitals, such as support of common hospital operations, long-term image archiving, secure image transmission among hospitals, and education and research support, we handle large databases of medical images (more than 2 million studies) [17–19]. For testing purposes, we performed experiments using 6000 selected images of our education database that contains about 60 000 medical images. More information about testing medical image database are provided in study [20]. Test images were of size 512×512 pixels from nine modalities: Angioscopy, Computed Radiography, Computed Tomography, Digital Radiography, Mammography, Magnetic Resonance, Radio fluoroscopy, Ultrasound and X-ray Angiography. Images were 8–16-bit, depending on the modality.

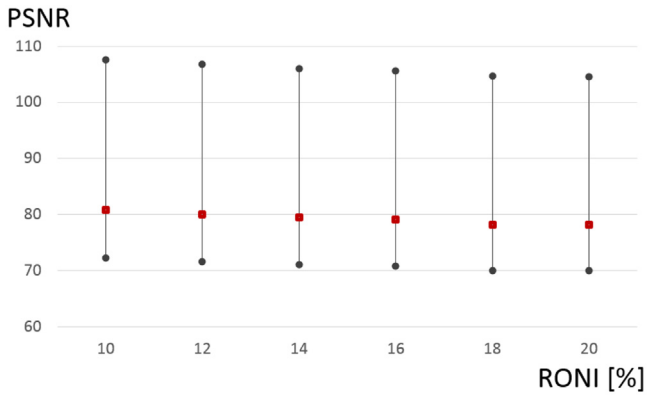

Fig. 18. Dependency of min, max and the average PSNR value on the size of RONI.

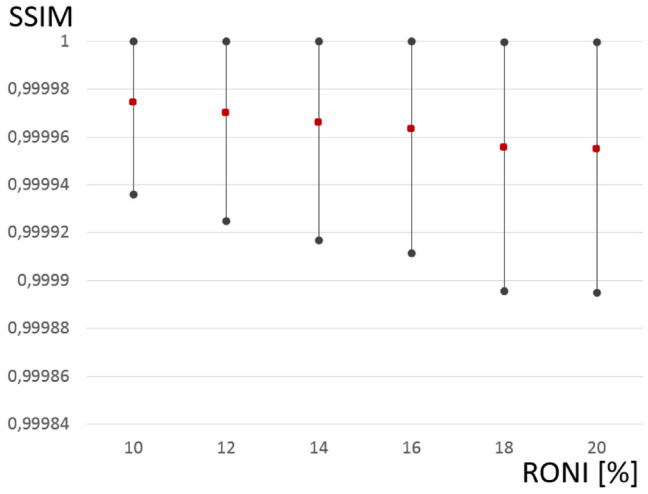

Fig. 19. Dependence of the minimum, maximum and average values of SSIM on the size of RONI.

The graph in Fig. 18 illustrates the dependency of min, max and the average PSNR value on the size of RONI. From the graph, it is evident that on the test images, PSNR was around 81. As expected, increasing RONI slightly decreases PSNR. The maximum value of PSNR was 107.6 at 10% of RONI. We have not seen such high values of PSNR on any published method.

Fig. 19 shows the dependence of the minimum, maximum and average values of SSIM on the size of RONI.

For all cases of RONI size, we found images which could be watermarked with SSIM 1.0. The average SSIM for images with RONI Size 10% is 0.999974. Increasing RONI decreases average SSIM to 0.999955 at 20% RONI size.

7.4. Comparison with other methods

In the graph in Fig. 20, there is a comparison of watermarking methods which use separation between ROI and RONI. The proposed method uses a novel approach, which requires a RONI size of only 10%, whereas 90% of the image – the ROI – remains unchanged. We were unable to find any methods in the available literature that would be directly comparable to that in the same work area.

Method [22] has a working area with RONI sizes in the range 76–79%, [23] 88–96%, and [24] has published results for different types of modalities at RONI size of 88%. To be able to compare, the proposed method was tested with RONI size over 10%. Comparing with other methods is also difficult due to the different character-

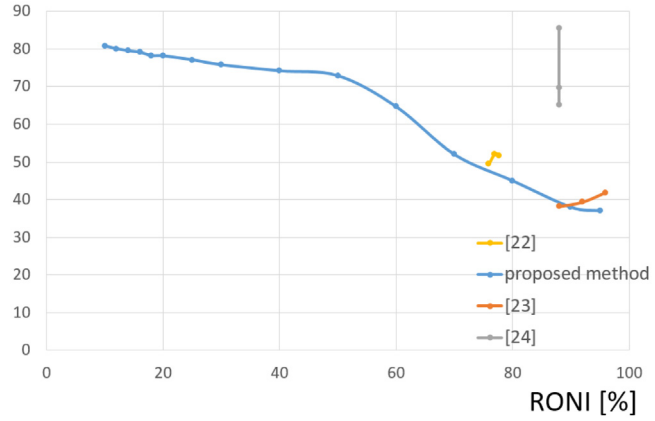

Fig. 20. Comparison of average PSNR valued of proposed method with other methods.

istics of each method. Some allow tamper detection, other have a high capacity for data hiding.

The proposed method assumes that if the medical image was modified or damaged, it loses its medical value. Such disruption is method able to detect. The proposed method focuses on the possibility of working with watermarked images (for diagnosis etc.) and the ability to be fully reversible. Because 90% of the image remains completely unchanged, the method achieves high PSNR. Test images on which were carried out practical experiments mostly had a bit-depth of 16 bits. A comparison of methods shows promising results for the proposed method.

8. Conclusion

This article describes a unique method of securing digital medical images that achieves exceptional results. The method combines the zero distortion of Zero-watermarking in ROI with the high capacity of Reversible watermarking in RONI. The average value of PSNR in images from the test database of 6000 medical images was 81, when RONI was 10% of the image size. In some cases, PSNR even exceeded 105. Another parameter, SSIM, which takes into account human perception of images, averages 0.999974. In the literature, we were unable to trace any watermarking method that achieved similar parameters and did not require storing additional information outside of the image itself. A comparison of the proposed method with other watermarking methods, which use separation of ROI and RONI, shows promising results.

Our next step will be a test on a larger medical image database, which will be ten times bigger, with images from various areas of medicine used in common hospital operation. This method eliminates the principal disadvantages of two common methods by carefully combining them in a way which can be fully automated. We will work to bring this method into practice.

Acknowledgements

This research was supported by FIONA Eureka LF14035. Computational resources were provided by the CERIT Scientific Cloud LM2015085.

References

[1] A. Roček, M. Javorník, Securing a publicly accessible database of medical images using watermarking with direct diagnose capability, Recent Adv. Comput. Sci. 13 (2014) 79–86, č. 24, s. ISSN 1790-5109.
[2] A. Roček, Medical image data security based on principles of digital watermarking methods. Malta, Adv. Data Netw. Commun. Comput. Mater. (2012) 47–52, stránky 978-1-61804-118-0.
[3] F. Rahimi, H. Rabbani, A dual adaptive watermarking scheme in contourlet domain for DICOM images, BioMed. Eng. Online (2011), 10:53 http://www.biomedical-engineering-online.com/content/10/1/53.
[4] O.M. Al-Qershi, B.E. Khoo, Authentication and data hiding using a hybrid ROI-based watermarking scheme for DICOM images, J. Digit. Imaging 24 (February (1)) (2011) 114–125.
[5] Ch. K. Tan, J. Ch. Ng, X. Xu, Ch. L. Poh, Y.L. Guan, K. Sheah, Security protection of DICOM medical images using dual-layer reversible watermarking with tamper detection capability, J. Digit. Imaging 24 (June (3)) (2011) 528–540.
[6] H. Rahmani, R. Mortezaei, M.E. Moghaddam, A new lossless watermarking scheme based on DCT coefficients, 6th International Conference on Digital Content, Multimedia Technology and its Applications (IDC) (2010) 28–33, ISBN: 978-1-4244-7607-7.
[7] H.H. Tsai, H.C. Tseng, Y.S. Lai, Robust lossless image watermarking based on a trimmed mean algorithm and support vector machine, J. Syst. Softw. 83 (2010) 1015–1028.
[8] W. Pan, G. Coatrieux, J. Montagner, N. Cuppens, F. Cuppens, Ch. Roux, Comparison of some reversible watermarking methods in application to medical images, in: 31st Annual International Conference of the IEEE EMBS, Minneapolis, Minnesota, USA, Sep. 2–6, 2009, pp. 2172–2175.
[9] I.F. Kallel, M.S. Bouhlel, J.Ch. Lapayre, Improved Tian's method for medical image reversible watermarking, GVIP J. vol. 7 (Aug (2)) (2007) 1–5.
[10] R. Fu, W. Jin, A Wavelet-Based Method of Zero-Watermark Utilizing Visual Cryptography, International Conference on Multimedia Technology (ICMT) (2010) 1–4, ISBN: 978-1-4244-7871-2.
[11] J.M. Zain, A.R.M. Fanzi, A.A. Aziz, Clinical evaluation of watermarked medical images, in: Proceedings of the 28th Annual International Conference of the IEEE EMBS, New York, 2006, pp. 5459–5462.
[12] Meryem Benyoussef, Samira Mabtoul, Mohamed El Marraki, Driss Aboutajdine, Robust image watermarking scheme using visual cryptography in dual-tree complex wavelet domain, J. Theor. Appl. Inf. Technol. 60 (2) (2014) 372–379, ISSN 1992-8645.
[13] Ivan W. Selesnick, Richard G. Baraniuk, Nick G. Kingsbury, The Dual-Tree Complex Wavelet Transform, vol. 5, IEEE Signal Processing Magazine, 2005, pp. 123–151.
[14] D. Coltuc, J.-M. Chassery, Very fast watermarking by reversible contrast mapping, IEEE Signal Process. Lett. 14 (4) (2007) 255–258, ISSN 1070-9908.
[15] N.V. Rao, V.M. Kumari, Watermarking in medical imaging for security and authentication, Inf. Secur. J.: Glob. Perspect. 20 (2011) 15–148, ISSN 1939-3555.
[16] Z. Wang, A.C. Bovik, H.R. Sheikh, E.P. Simoncelli, Image quality assessment: from error visibility to structural similarity, IEEE Trans. Image Process. 13 (April (4)) (2004) 600–612.
[17] K. Slavicek, M. Javornik, O. Dostal, Extension of the shared regional PACS center MeDiMed to smaller healthcare institutions, in: The Eleventh International Conference on Networks, Saint Gilles, Reunion Island, IARIA, 2012, pp. 83–87, ISBN 978-1-61208-183-0.
[18] M. Javornik, O. Dostal, K. Slavicek, Regional medical imaging system, World Acad. Sci. Eng. Technol. France 7 (79) (2011) 389–393, ISSN 2010-376X.
[19] O. Slavicek, M. Dostal, MEDIMED—regional centre for medicine image data processing, in: IEEE Computer Society: Knowledge Discovery and Data Mining, Phuket, Thailand 2010, pp. 310–313, ISBN 978-0-7695-3923-2.
[20] A. Roček, K. Slavíček, M. Javorník, RONI size and another attributes of representative sample of medical images in common hospital operation, related to securing by watermarking methods, in: International Conference on Image Processing, Production and Computer Science, London, 2016, pp. 44–51, ISBN 978-93-84422-62-2.
[21] J. Mašek, R. Burget, J. Karásek, V. Uher, S. Güney, Evolutionary improved object detector for ultrasound images, 36th International Conference on Telecommunications and Signal processing (2013) 586–590, 978-1-4799-0402-0.
[22] R. Eswaraiah, E.S. Reddy, Robust medical image watermarking technique for accurate detection of tampers inside region of interest and recovering original region of interest, IET Image Process. 9 (8) (2015) 615–625, ISSN 1751-9659.
[23] O.M. Al-Qershi, B.E. Khoo, ROI–based tamper detection and recovery for medical images using reversible watermarking technique, in: IEEE International Conference on Information Theory and Information Security, Beijing 2010, pp. 151–155, ISBN 978-1-4244-6942-0.
[24] O.M. Al-Qershi, B.E. Khoo, Authentication and data hiding using a hybrid ROI-based watermarking scheme for DICOM images, J. Digit. Imaging 24 (1) (2011) 114–125, ISSN 0897-1889.